

58-54

187839

p. 8

N94-19473

Efficiency and Biofidelity of Occupant Simulations

Walter D. Pilkey
University of Virginia
Charlottesville, VA

R AND G PARAMETERS: ATB SIMULATOR UNLOADING BEHAVIOR

This figure demonstrates how unloading is handled in the ATB occupant simulator for contact planes and seatbelts. Two parameters, R and G, are specified. R is the ratio of rebound energy to initial energy and G is the ratio of permanent deformation to maximum deformation. The program unloads along a quadratic curve which intersects the x-axis at D1, the point defined by G. The quadratic function is chosen to match the requested value of R as closely as possible while satisfying the G condition exactly. This puts an upper limit on R, which for linear loading and unloading is seen to be 1.0 G. Excessive rebound energy from the seatbelts prompted an investigation of the program's sensitivity to these parameters.

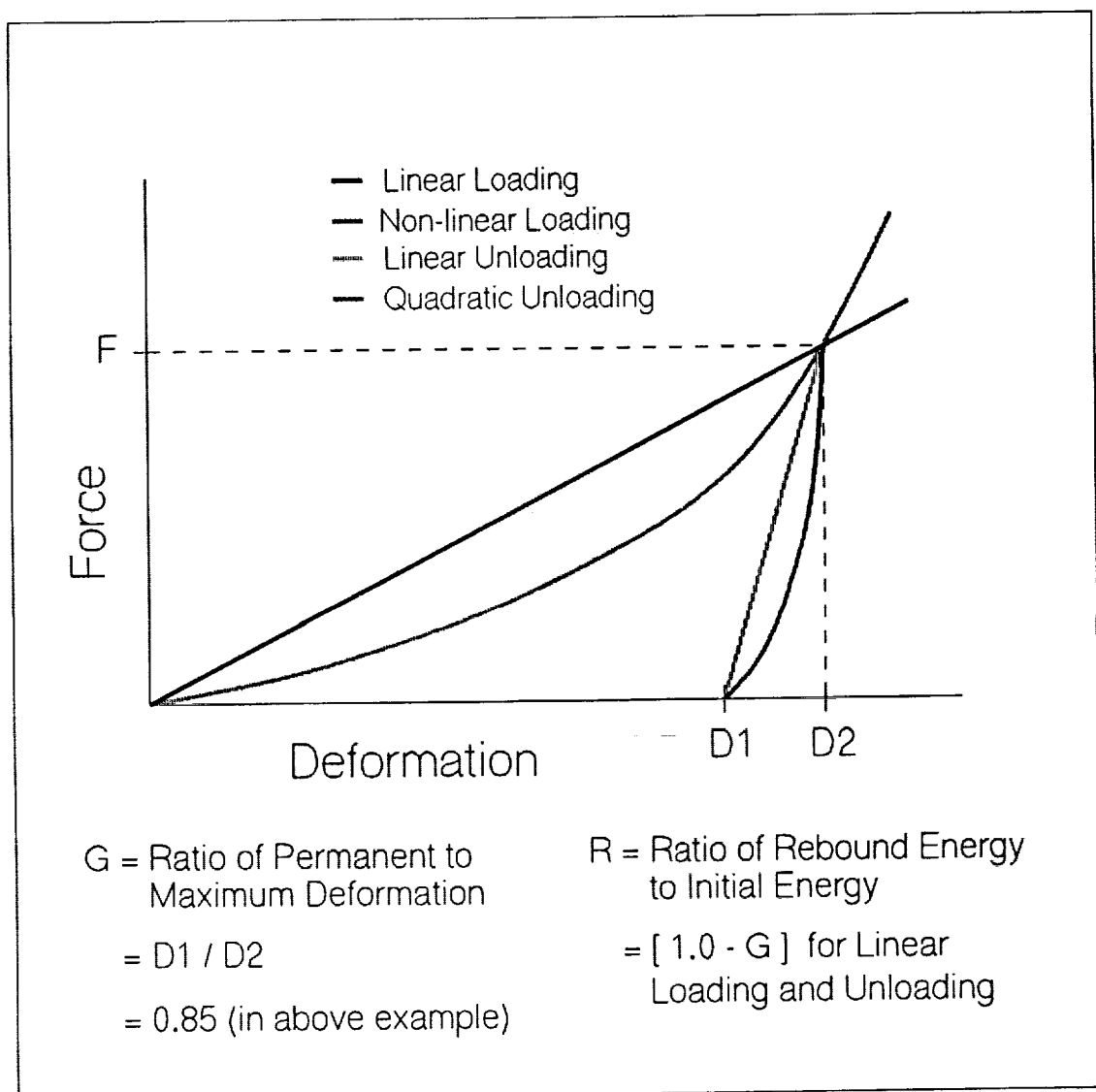


Figure 1

MOTION OF SPHERE RELATIVE TO VEHICLE AFTER VEHICLE DECELERATES

The sketch at the top of this figure shows an ATB model developed by the consulting firm, David James, Ltd. It is simply a sphere, restrained by a single belt, and sliding on a frictionless, decelerating plane (or vehicle). From their study they concluded that the ATB R and G parameters were essentially nonfunctional for the seatbelt. They passed their results on to UVA where initial simulations seemed to confirm their conclusions. However, changing the integration step-size caused a significant change in the results, particularly in the rebound energy of the sphere. A systematic study of step-size sensitivity was undertaken. The sketch at the bottom shows an equivalent restraint situation with the belt replaced by a contact plane. This model was used for comparison to the belt model.

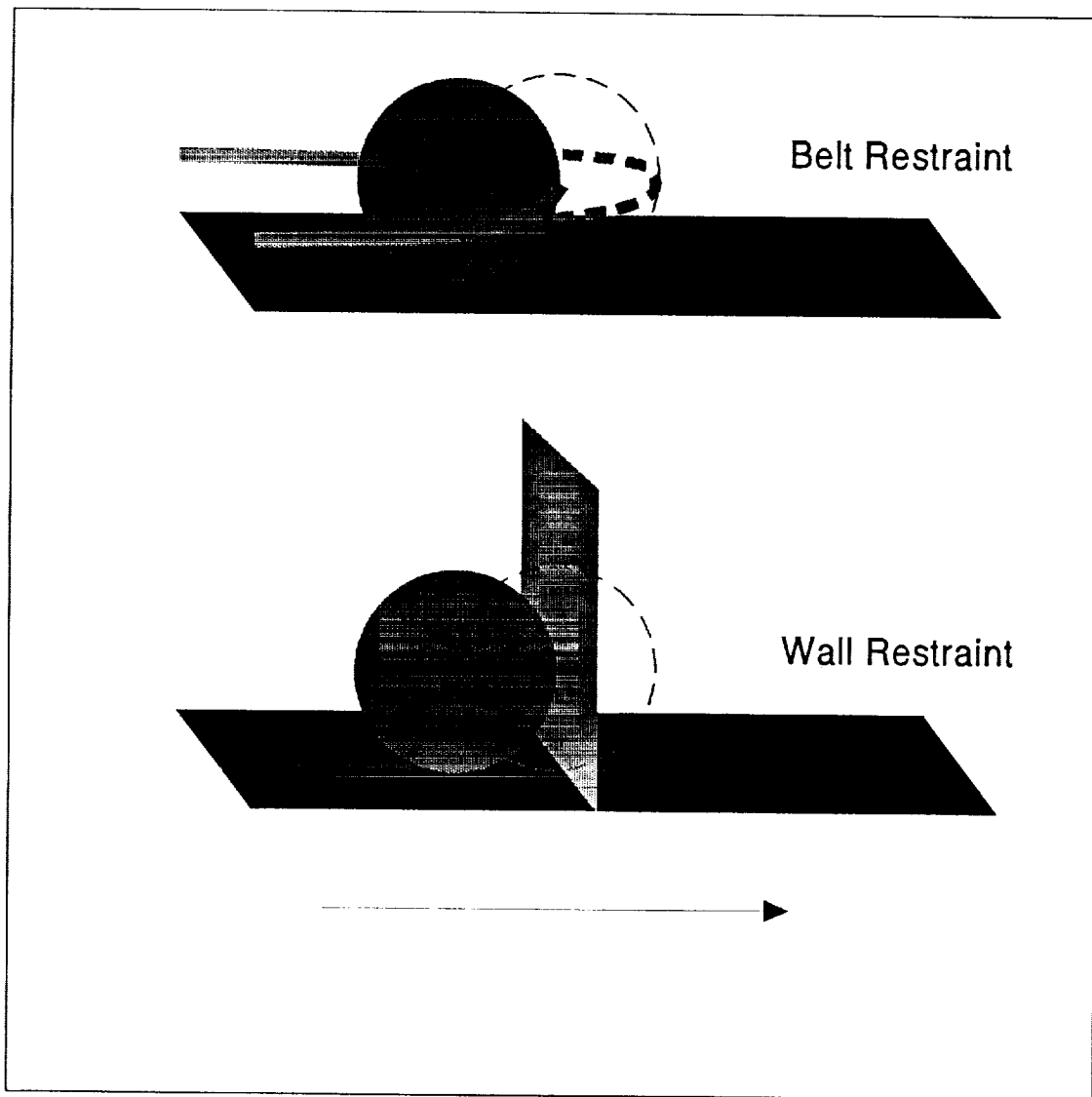


Figure 2

SPHERE DATA FOR BELT RESTRAINT

This figure displays the family of curves that were generated by lowering the integration step-size from 1.0 msec (the value used in the initial R and G investigation) to 0.01 msec. The G value was 0.85. As the 1.0 msec curve shows, the final rebound velocity is indeed greater than the maximum forward velocity. The energy return for the smallest step-size, however, is approximately 0.16, which is near the maximum for linear loading and unloading. Furthermore, the curves do appear to be converging. Unfortunately, the step-size required for convergence is extremely small, much smaller than is normally necessary for motion of an unbelted occupant. The conclusion of this study is that the belt algorithm does work, including the R and G parameters, but very small step-sizes are needed to get reasonable results.

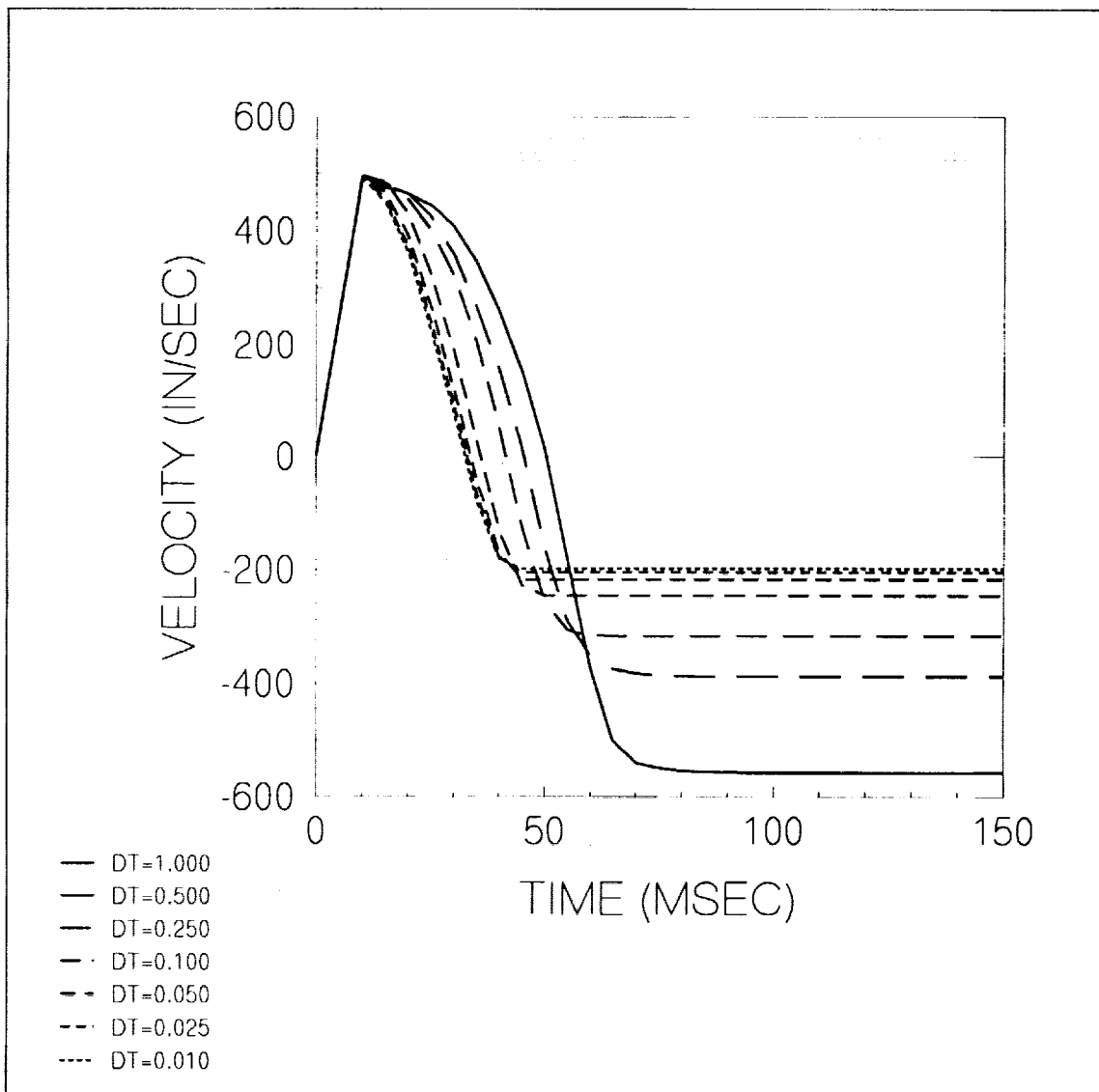


Figure 3

SPHERE DATA FOR WALL IMPACT

To check that the integration problems were limited to the seatbelt, an equivalent model was set up, as described in Fig. 2, with the belt replaced by a contact plane (or wall). This figure shows that the wall impact results are nearly identical to the best belt results and that there is no discernable difference between the wall results for 1.0 msec and for 0.01 msec. In fact, the two cases exhibited four-digit agreement. Thus, the basic integration method is apparently sound and problems are limited to the belt algorithm.

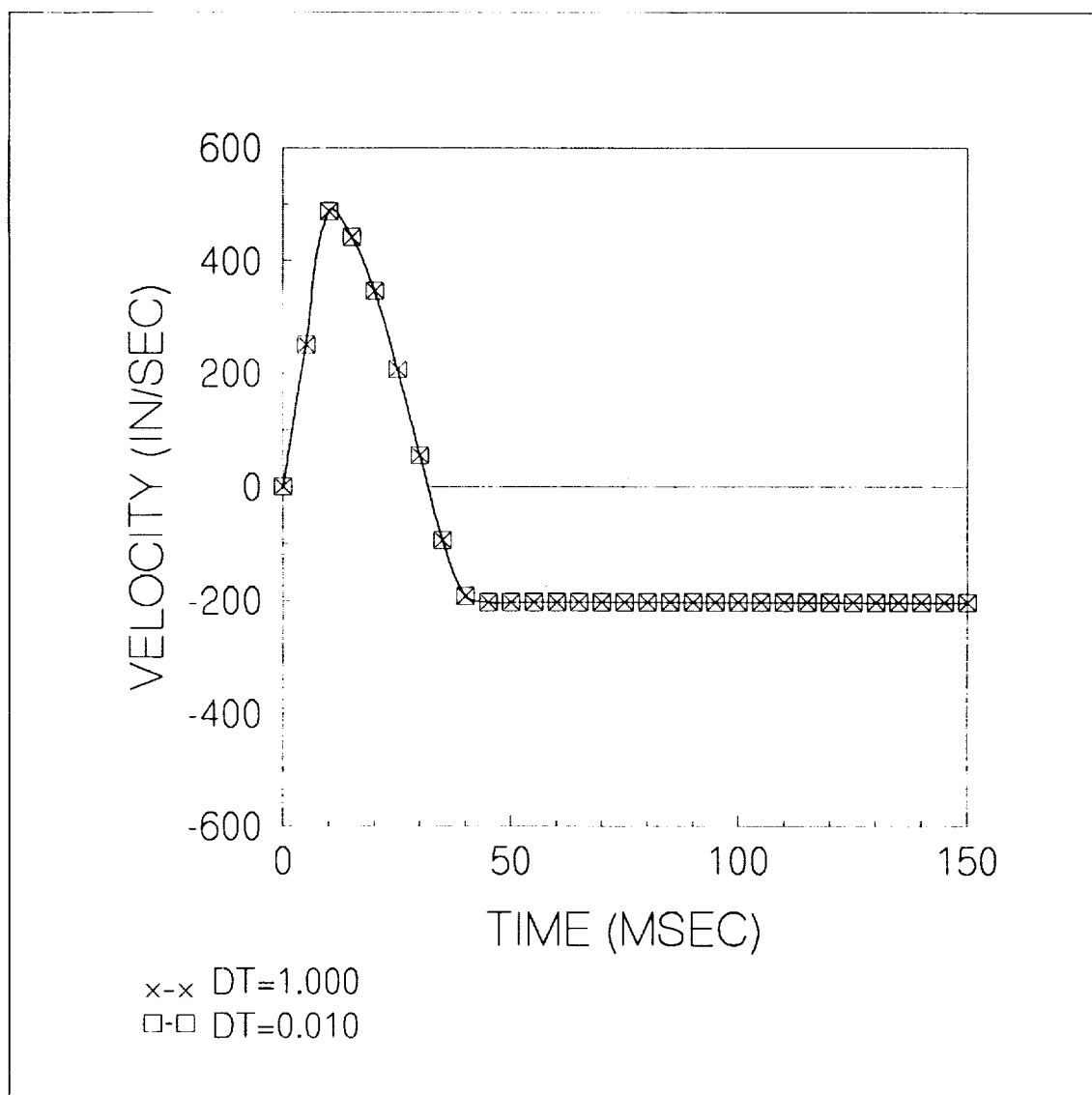


Figure 4

HEAD ACCELERATION VS. BELT SLACK X-DIRECTION (MEASURED)

This figure shows head acceleration curves from two UVA impact sled tests which used the same parameters except for the amount of slack in the shoulder belt. Of particular interest is the secondary peak that occurs near 85 msec for the curve generated by the run with 3 inches of slack. This peak had been noticed before in sled tests and in simulations, but had been considered not to have any significance since its magnitude was always much lower than that of the primary peak. It appears, however, that the secondary peak may be associated with experimental parameters such as belt slack. Thus, while they are not of great importance from the standpoint of injury prediction, this and other secondary features have the potential to be of useful diagnostic value if their appearance in the pulse can consistently be associated with known parameters.

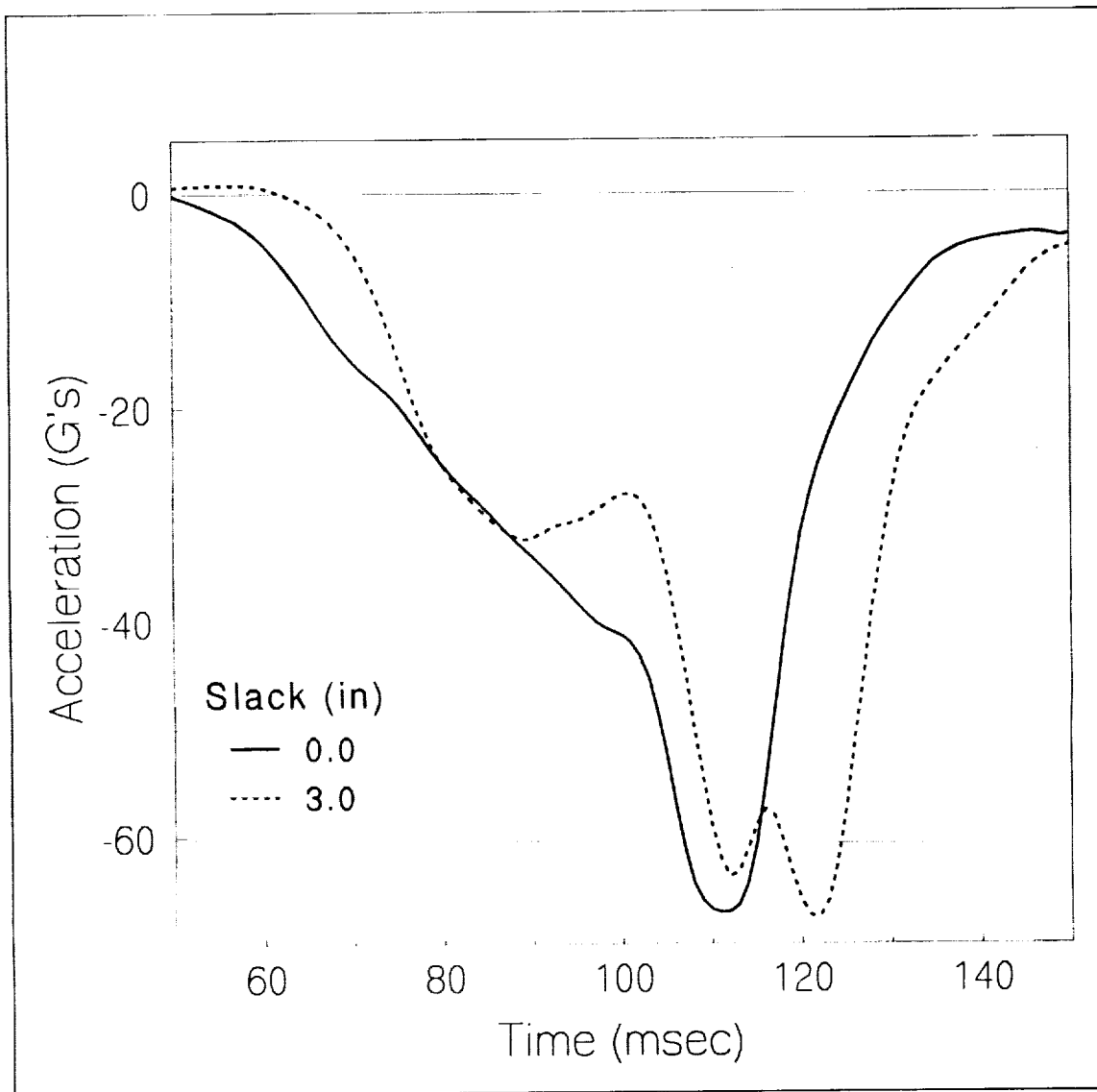


Figure 5

HEAD ACCELERATION VS. BELT SLACK X-DIRECTION (SIMULATED)

This figure shows ATB simulator results which are similar to the sled measurements. The shape and timing of the pulses need some improvement before they are compared directly to the sled results, but the appearance of a secondary peak resulting from the introduction of belt slack is clearly demonstrated.

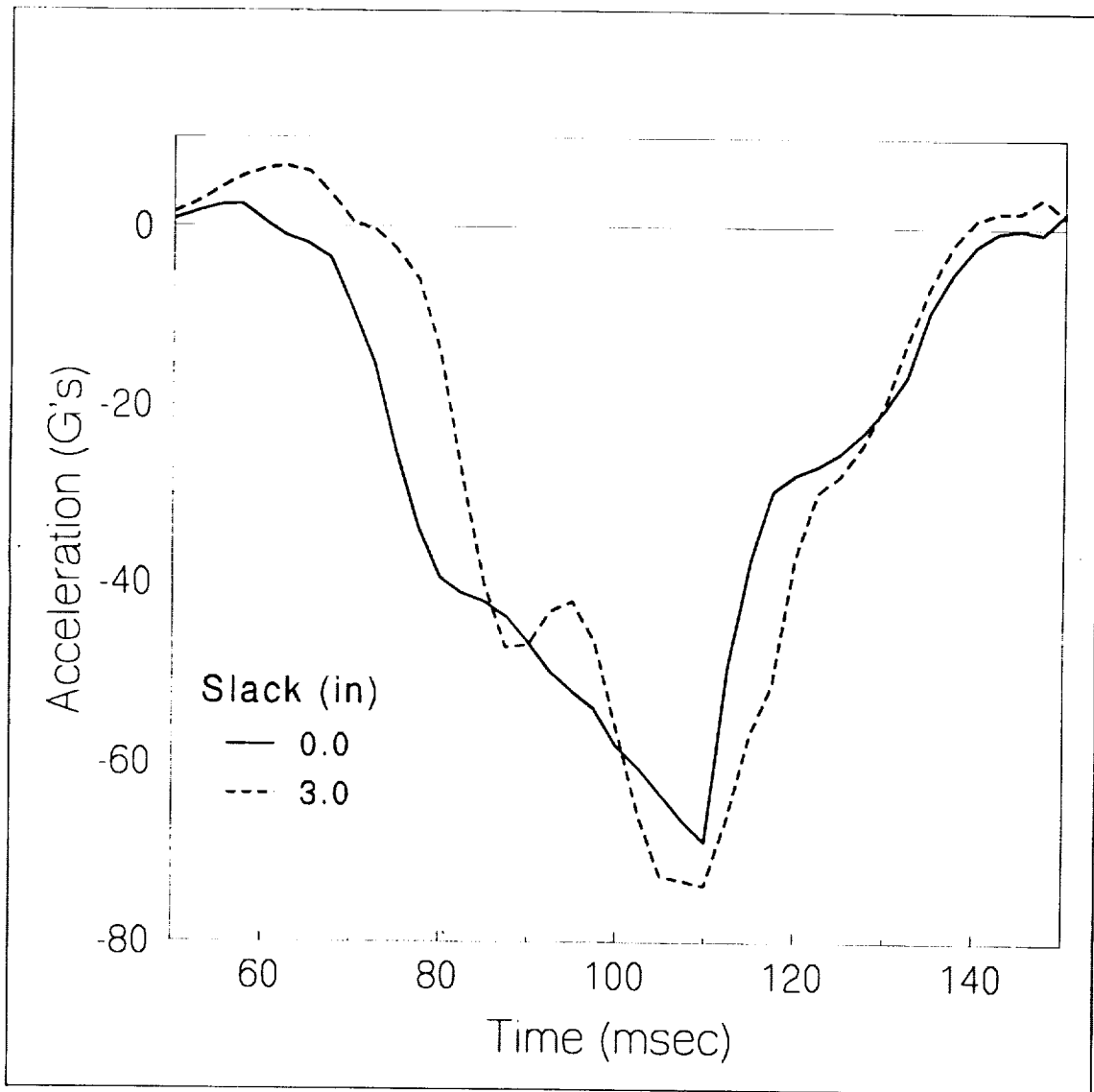


Figure 6

HEAD ACCELERATION VS. BELT SLACK X-DIRECTION (SIMULATED)

This figure shows that the secondary peak is not an anomaly associated with a particular value of belt slack. It appears for higher and lower values as well, and demonstrates a predictable sensitivity to the amount of slack. Note that it shows greater sensitivity to the slack parameter than does the primary peak, particularly in terms of timing and the depth from the peak to the following trough. This increased sensitivity may be exploitable when diagnosing test results.

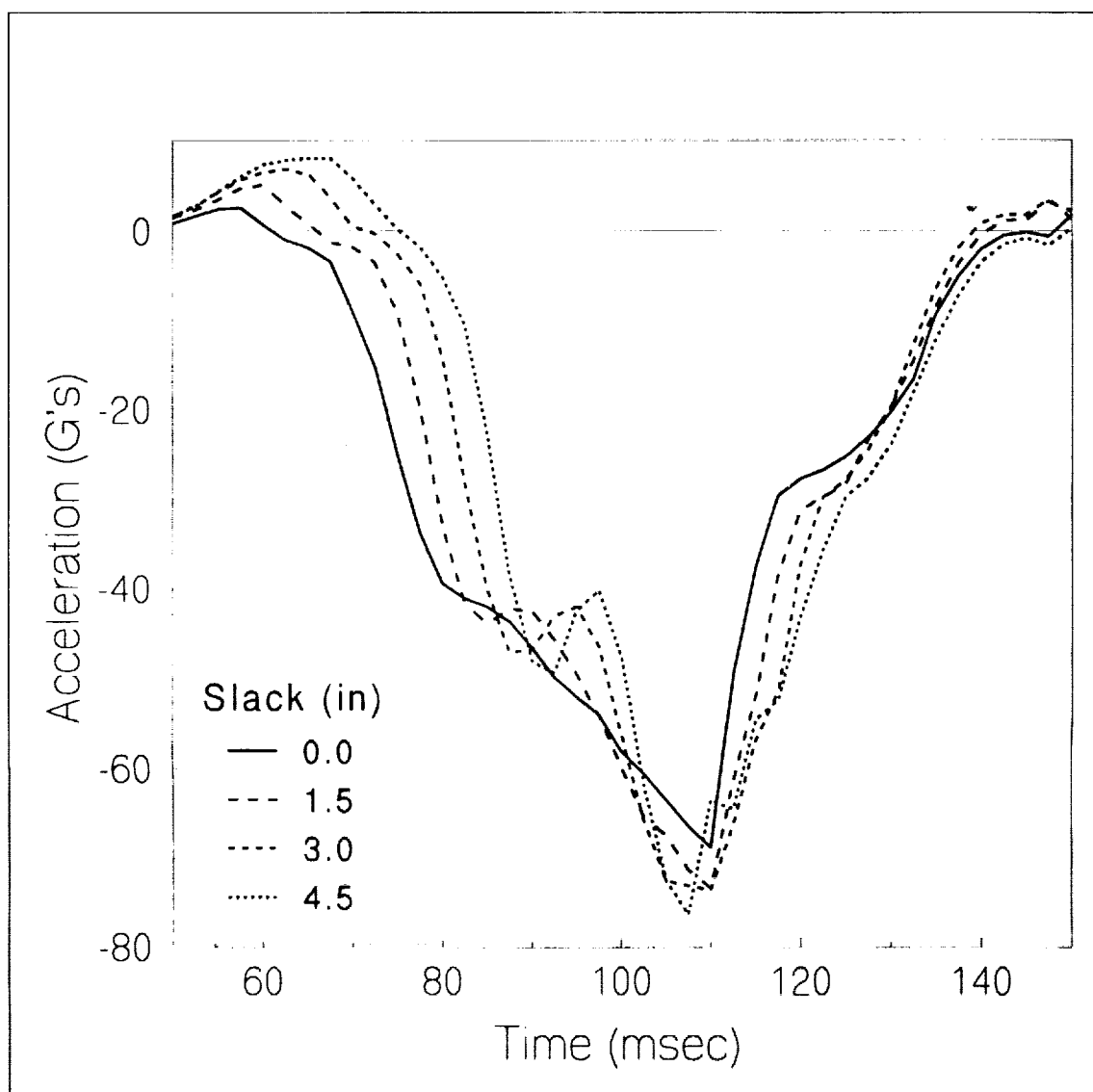


Figure 7

